5. CONCLUSION

Detailed design of a penta-band antenna, which is comprised of two folded inverted-L radiators and one matching arm, is presented in this paper. The results of the parametric study, investigation of the current distributions, and the effects of the ground plane and hand on the proposed antenna have been included. The designed antenna has two main bands, the first of which covers the GSM 900 band, whereas the other operates in DCS, PCS, UMTS, and Bluetooth bands. Simulation results show that these two bands can be controlled relatively independently within certain limitation. The experimental results show that the frequency with range in the return loss better than 7.5 dB covers the range 830–1010 MHz in the low band and 1710 MHz to higher than 2600 MHz at the high band. A study of the current distribution on the ground plane indicates that large currents are concentrated near the ground plane portion very close to the location of the antenna. One consequence of this is that, even if a small change the region below affects the return loss significantly. However, relatively larger modification in the opposite side of the ground plane has little effect on the return loss. As far as the hand effects on the performance of the antenna are concerned, it was found that the total efficiency decreases significantly when the human hand grips the mobile phone, especially when the hand is close to the antenna, and the total efficiency declines from near 90% to around 40% within all operating bands in this situation. The preferable position for the antenna in the mobile phone is far away from the position where the consumers typically grip the phone.

ACKNOWLEDGMENTS

This work was carried out in collaboration with Advanced Antenna Group in Samsung and was supported in part by the university-level project of Communication University of China under Grant XNG1106.

REFERENCES

1. D. Kim, J. Lee, C. Cho, and T. Lee, Design of a compact tri-band PIFA based on independent control of the resonant frequencies, IEEE Trans Antennas Propag 56 (2008), 1428–1436.
2. H.F. AbuTarboush, R. Nilavalan, T. Peter, and S.W. Cheung, Multiband inverted-F antenna with independent bands for small and slim cellular mobile handsets, IEEE Trans Antennas Propag 59 (2011), 2636–2645.
3. S.H. Yeh, K.L. Wong, T.W. Chiou, and S.T. Fang, Dual-band planar inverted F antenna for GSM/DCS mobile phones, IEEE Trans Antennas Propag 51 (2003), 1124–1126.
4. R.A. Bhatti, Y.T. Im, J.H. Choi, T.D. Manh, and S.O. Park, Ultrathin planar inverted-F antenna for multistandard handsets, 2894–2897.
5. T.Y. Wu and K.L. Wong, On the impedance bandwidth of a planar inverted-F antenna for mobile handsets, Microwave Opt Technol Lett 32 (2002), 249–251.
6. C.H. Chang and K.L. Wong, Printed λ/8-PIFA for penta-band WWAN operation in the mobile phone, IEEE Trans Antennas Propag 57 (2009), 1373–1381.
7. Y.L. Kuo and K.L. Wong, Coplanar waveguide-fed folded inverted-F antenna for UMTS application, Microwave Opt Technol Lett 32 (2002), 364–366.
8. S.-Y. Lin, Multiband folded planar monopole antenna for mobile handset, IEEE Trans Antennas Propag 52 (2004), 1790–1794.
9. J.H. Chen, C.J. Ho, C.H. Wu, S.Y. Chen, and P.W Hsu, Dual-band planar monopole antenna for multiband mobile systems, IEEE Antennas Wireless Propag Lett 7 (2008), 769–772.
10. Y.S. Shin, S.O. Park, and M.J. Lee, A broadband interior antenna of planar monopole type in handsets, IEEE Antennas Wireless Propag Lett 4 (2005), 9–12.
11. C.M. Peng, I.F. Chen, and C.T. Chien, A novel hexa-band antenna for mobile handsets application, IEEE Trans Antennas Propag 59 (2011), 3427–3431.
12. M.C. Huynh and W. Stutzman, Ground plane effects on planar inverted-F antenna (PIFA) performance, IEE Proc Microwave Antennas Propag 150 (2003), 209–213.
13. S. Noghanian and L. Shafai, Control of microstrip antenna radiation characteristics by ground plane size and shape, IEE Proc Microwave Antennas Propag 145 (1998), 207–212.
14. Y.X. Guo, K.M. Luk, and K.F. Lee, L-probe fed thick-substrate patch antenna mounted on a finite ground plane, IEEE Trans Antennas Propag 51 (2003), 1955–1963.
15. M.A. Jensen and Y. Rahamat-Samii, EM interaction of handset antennas and a human in personal communication, Proc IEEE 83 (1995), 7–17.
16. C.H. Li, E. Ofli, N. Chavannes, and N. Kuster, Effects of hand phantom on mobile phone antenna performance, IEEE Trans Antennas Propag 57 (2009), 2763–2770.
17. J. Ilvonen, O. Kivekas, J. Holopainen, R. Valkonen, K. Rasilainen, and P. Vainikainen, Mobile terminal antenna performance with the user's hand: Effect of antenna dimensioning and location, IEEE Antennas Wireless Propag Lett 10 (2011), 772–775.
18. C. Gabriel, Tissue equivalent material for hand phantoms, Phys Med Biol 52 (2007), 4205–4210.

WWAN PRINTED MONOPOLE SLOT ANTENNA WITH A PARALLEL-RESONANT SLIT FOR TABLET COMPUTER APPLICATION

Kin-Lu Wong and Wun-Jian Lin
Department of Electrical Engineering, National Sun Yat-Sen University, Kaohsiung 804, Taiwan, Republic of China; Corresponding author: wongkl@ema.ee.nsysu.edu.tw

Received 6 April 2012

ABSTRACT: *The use of a parallel-resonant (PR) slit for dual-band bandwidth enhancement of a small-size printed monopole slot antenna to achieve the wireless wide area network operation in the tablet computer is demonstrated. The antenna is easy to fabricate by printing on a thin FR4 substrate of size 10 × 45 mm^2. The PR slit, mainly configured as a spiral shape to occupy a small area of about 6.5 × 6.5 mm^2 on the FR4 substrate, generates two parallel resonances at about 1.2 and 2.5 GHz to, respectively, result in dual-resonance excitation of the quarter-wavelength and half-wavelength modes of the monopole slot at about 0.9 and 1.9 GHz. In this case, two wide operating bands are obtained to, respectively, cover the 824–960 and 1710–2170 MHz bands. That is, with the dual-band bandwidth enhancement contributed by the PR slit, the proposed antenna can cover the GSM850/900/1800/1900/UMTS bands with a small planar size. Details of the proposed antenna are described in the article.* © 2012 Wiley Periodicals, Inc.

Microwave Opt Technol Lett 55:40–45, 2013; View this article online at wileyonlinelibrary.com. DOI 10.1002/mop.27273

Key words: *mobile antennas; tablet computer antennas; WWAN antennas; printed slot; Antennas; parallel-resonant slit*

1. INTRODUCTION

Recently, it has been shown that by applying a parallel-resonant (PR) spiral slit, a small-size planar tablet computer antenna can provide two wide operating bands to cover the 824–960 and 1710–2170 MHz for penta-band wireless wide area network (WWAN) operation [1]. The applied PR slit generally does not increase the size of the antenna, and the wideband operation is

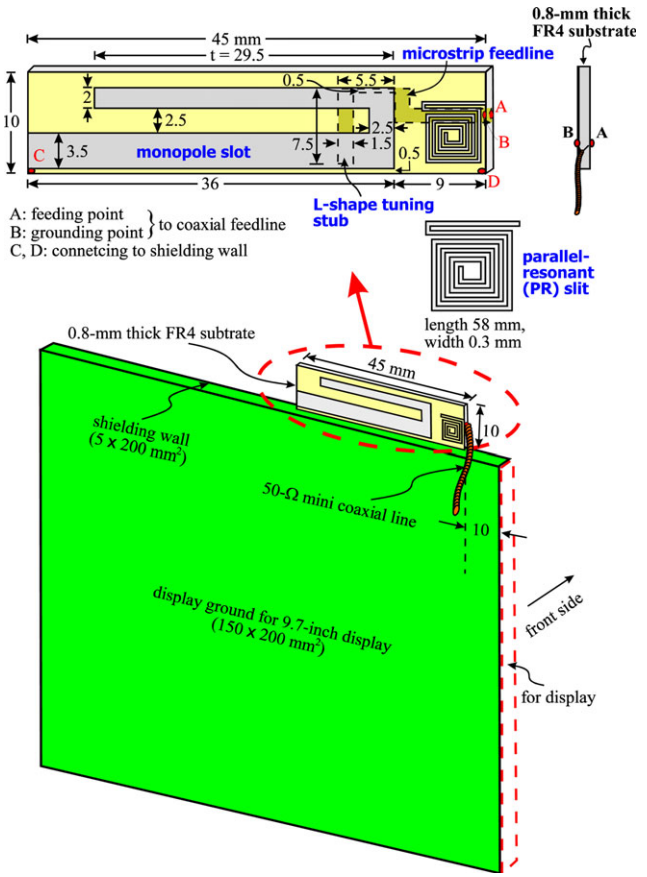

Figure 1 Geometry of the WWAN printed monopole slot antenna with a parallel-resonant slit for tablet computer application. [Color figure can be viewed in the online issue, which is available at wileyonlinelibrary.com]

obtained by generating a parallel resonance [2–7] at about 1.2 GHz, higher than the antenna's desired lower band, to cause a new resonance occurred inside the desired lower band and nearby the originally excited resonant mode of the antenna at about 850 MHz. This feature leads to a dual-resonance characteristic obtained for the antenna's lower band, making it capable of wideband operation to cover the desired 824–960 MHz band with a small antenna size. To achieve such a parallel resonance, the technique of using a band-stop circuit which comprises a chip inductor and a chip capacitor connected in series [2–5] or using a distributed band-stop circuit which comprises a printed shorted strip to closely couple with the antenna's main radiator [6, 7] has been applied. In the latter case, the printed shorted strip contributes an equivalent inductance to perform as a printed inductor, whereas the coupling between the shorted strip and the antenna's main radiator contributes an equivalent capacitor to perform as a printed capacitor, both the printed inductor and capacitor formed into a printed PR circuit for the antenna to generate a parallel resonance at the desired frequency. However, the results shown in Refs. 1–7 that have been reported can effectively lead to the widening of the antenna's lower band only.

In this article, we report the design of using a PR slit to generate two parallel resonances at about 1.2 and 2.5 GHz to, respectively, help enhance the lower-band and upper-band bandwidths of the antenna to cover the 824–960 and 1710–2170 MHz bands for the penta-band WWAN operation. The PR slit is applied to a simple folded monopole slot antenna [8–15], which contributes its quarter-wavelength and half-wavelength slot modes. With the proposed design, the antenna is easy to fabricate at low cost by printing on a thin FR4 substrate of small size (10 × 45 mm^2). The antenna is especially suitable for tablet computer applications, and the obtained results are presented and discussed.

2. PROPOSED ANTENNA

Figure 1 shows the geometry of the WWAN printed monopole slot antenna with a PR slit for tablet computer application. Figure 2 shows photos of the fabricated prototype. As shown in Figure 1, the antenna is mounted along the top shielding metal wall (size 5 × 200 mm^2) of the display ground of the tablet computer. The size of the display ground is selected to be 150 × 200 mm^2 to accommodate a 9.7-inch display, which is commonly applied for practical tablet computers. The antenna is printed on a 0.8-mm thick FR4 substrate of size 10 × 45 mm^2, relative permittivity 4.4, and loss tangent 0.024, which is inexpensive and makes the antenna easy to fabricate at low cost.

The monopole slot antenna is folded to achieve a compact configuration and has a length of 73.5 mm along its outer boundary. The slot length is close to a quarter-wavelength at 850 MHz. The monopole slot is excited by a microstrip feedline printed on the opposite surface where the monopole slot is printed. Note that the open stub of the microstrip feedline facing the monopole slot is configured to be an L-shaped stub of various widths to achieve good excitation of the quarter-wavelength and half-wavelength resonant slot modes. The PR slit is configured to be about a spiral shape and occupies a small area of about 6.5 × 6.5 mm^2 on the FR4 substrate. Both the monopole slot and PR slit are printed on the same surface, and the PR slit also faces the microstrip feedline on the opposite surface of the substrate.

To feed the antenna for the tablet computer application, a 50-Ω coaxial feedline is applied, with its central conductor connected to the microstrip feedline and its outer grounding sheath connected to the ground plane on the substrate surface where the monopole slot and PR slit are printed. Note that when the

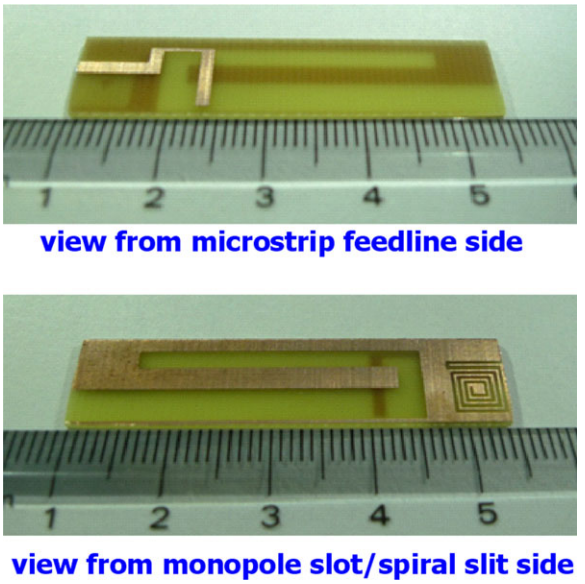

Figure 2 Photos of the fabricated antenna. [Color figure can be viewed in the online issue, which is available at wileyonlinelibrary.com]

PR slit is not present, the excited quarter-wavelength and half-wavelength slot modes contributed by the monopole slot are of narrow bands and cannot cover the desired 824–960 and 1710–2170 MHz bands [16–19]. With the presence of the PR slit, two parallel resonances at about 1.2 and 2.5 GHz are generated. The occurrences of the two parallel resonances can be controlled by tuning the length of the PR slit, which is selected to be 58 mm in this study. By decreasing the length of the PR slit, the generated parallel resonances can be shifted to higher frequencies. The related dependence of the generated parallel resonances on the length of the PR slit will be analyzed in Section 3. The two parallel resonances can, respectively, result in the generation of a new resonance (zero reactance) close to the excited quarter-wavelength and half-wavelength slot modes. This behavior leads to two operating bands with dual-resonance characteristic to have much widened bandwidths. The antenna can hence cover the desired penta-band WWAN operation by using a simple folded monopole slot antenna with a small occupied size.

3. RESULTS OF FABRICATED ANTENNA

The antenna was fabricated as shown in Figure 2 and was tested in the configuration as shown in Figure 1. Results of the measured and simulated return loss of the antenna are presented in Figure 3. The shaded region in the figure indicates the desired lower and upper bands for the WWAN operation. For frequencies over the desired operating bands, the measured impedance matching is better than 3:1 VSWR or 6-dB return loss, which is widely used as the design specification of the internal mobile device antennas. Also note that the simulated results obtained using high frequency structure simulator [20] agree well with the measured data shown in figure.

Figure 4 shows the measured antenna efficiency of the antenna. The antenna efficiency shown in figure includes the mismatching loss. The antenna efficiency is about 55–70% and 53–72% over the lower and upper bands, respectively. The measured radiation patterns of the antenna at representative frequencies are plotted in Figure 5. At lower frequencies (859 and 925 MHz, central frequencies of the GSM850 and GSM900 bands), omnidirectional radiation or near-omnidirectional radiation is seen in the azimuthal plane (x-y plane), which is similar to those observed at about 900 MHz for the internal handset antennas [21–28]. This suggests that although the display ground in this study is larger than the system ground plane of the handset, the display ground is still a part of the radiator and contributes to some radiation at lower frequencies. At higher frequencies (1795, 1920, and 2045 MHz, central frequencies of the GSM1800, GSM1900, and UMTS bands), however, asymmetric radiation patterns are seen. The radiation in the $+y$ direction is much stronger than that in the $-y$ direction, which is due to the antenna mounted close to one corner of the top shielding metal wall. This arrangement is for the purpose of accommodating more possible antennas along the top shielding metal wall for practical applications in which other antennas are generally required to be embedded in the tablet computers.

Detailed operating principle of the proposed antenna is also analyzed. Figure 6 shows the simulated return loss for the proposed antenna with and without the PR slit. The antenna geometry for the case without the PR slit (Ant1) is also shown in

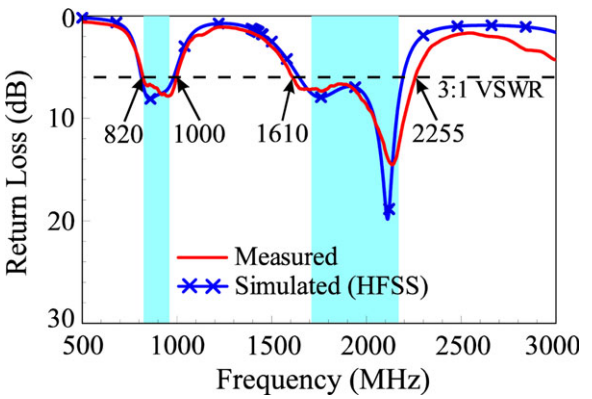

Figure 3 Measured and simulated return loss of the proposed antenna. [Color figure can be viewed in the online issue, which is available at wileyonlinelibrary.com]

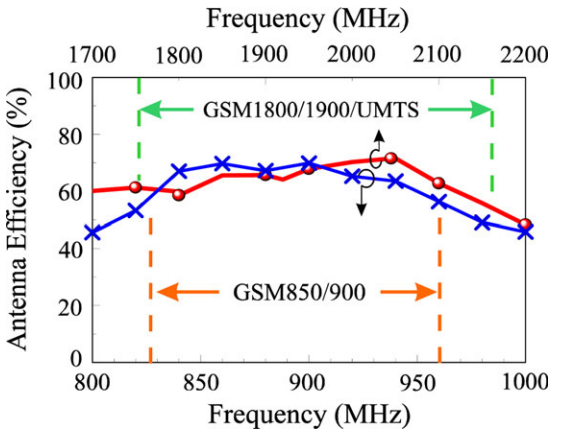

Figure 4 Measured antenna efficiency (mismatching loss included) of the proposed antenna. [Color figure can be viewed in the online issue, which is available at wileyonlinelibrary.com]

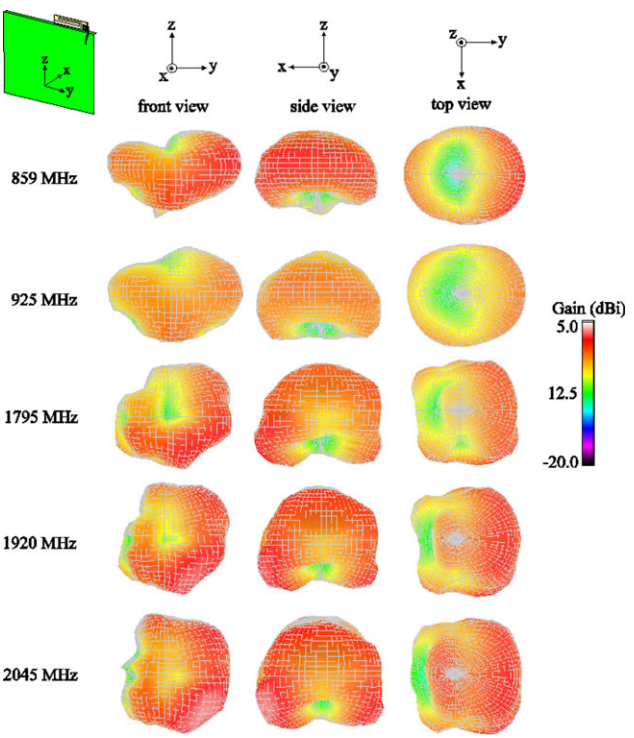

Figure 5 Measured radiation patterns of the proposed antenna. [Color figure can be viewed in the online issue, which is available at wileyonlinelibrary.com]

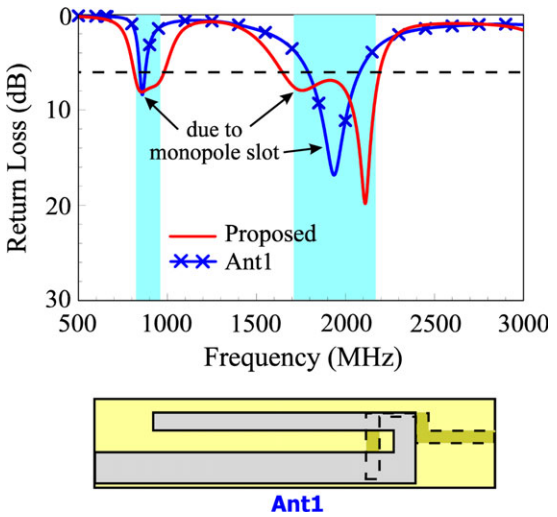

Figure 6 Simulated return loss for the proposed antenna with and without the PR slit. [Color figure can be viewed in the online issue, which is available at wileyonlinelibrary.com]

figure. It is seen that without the presence of the PR slit, the two excited resonant modes at about 850 and 1900 MHz are of narrow bandwidths. The corresponding results of the simulated input impedance of the proposed antenna and Ant1 are also presented in Figure 7. Two parallel resonances excited at about 1.2 and 2.5 GHz are clearly seen. The lower parallel resonance leads to the generation of a new resonance at about 900 MHz, which combines with the quarter-wavelength slot mode at about 850 MHz to result in a dual-resonance operating band for the antenna's lower band. Similarly, the higher parallel resonance leads to the generation of a new resonance at about 2 GHz, which combines with the half-wavelength slot mode to result in a dual-resonance upper band for the antenna. Two wide operating bands are hence obtained for the antenna, and the desired 824–960 and 1710–2170 MHz bands are covered.

To further identify the excitation of the slot modes and the parallel resonances, Figure 8 shows the simulated electric field distributions in the monopole slot and the PR slit. At 850 and

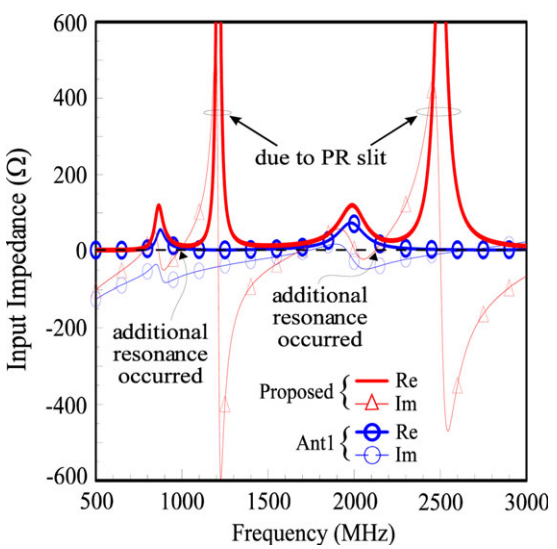

Figure 7 Simulated input impedance for the two antennas studied in Fig. 6. [Color figure can be viewed in the online issue, which is available at wileyonlinelibrary.com]

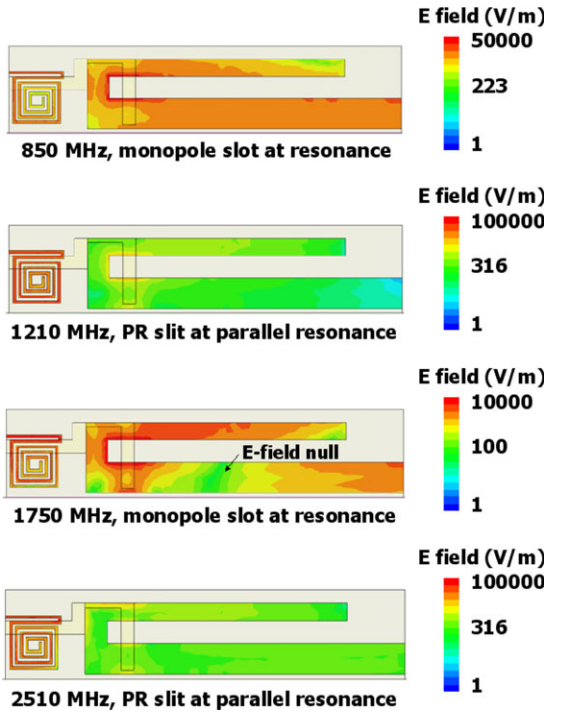

Figure 8 Simulated electric field distributions in the monopole slot and the PR slit. [Color figure can be viewed in the online issue, which is available at wileyonlinelibrary.com]

1750 MHz, the first mode in the antenna's lower and upper bands as shown in Figure 6, the excited electric field distributions in the monopole slot indicate that the slot modes are excited. At 850 MHz, the slot mode is a quarter-wavelength mode, whereas at 1750 MHz, it is a half-wavelength mode (see an E-field null in the monopole slot). At 1210 and 2510 MHz, it is clearly seen that the PR slit is excited, whereas the monopole slot is not excited. This confirms that the PR slit indeed generates parallel resonances at about 1.2 and 2.5 GHz, which in turn results in the dual-resonance lower and upper bands for the proposed antenna.

The parallel resonances can also be controlled by tuning the length of the PR slit. Figure 9 shows the simulated input resistance as a function of the slit length. It is seen that both the lower and higher parallel resonances occurs at increasing frequencies with decreasing length of the PR slit, indicating that the parallel resonances can indeed be controlled by the length of the PR slit.

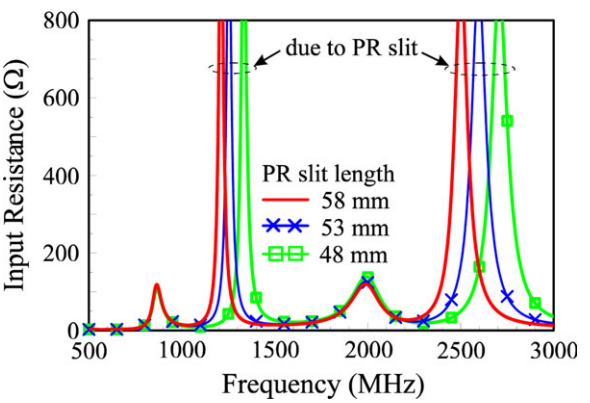

Figure 9 Simulated input resistance as a function of the length of the PR slit. [Color figure can be viewed in the online issue, which is available at wileyonlinelibrary.com]

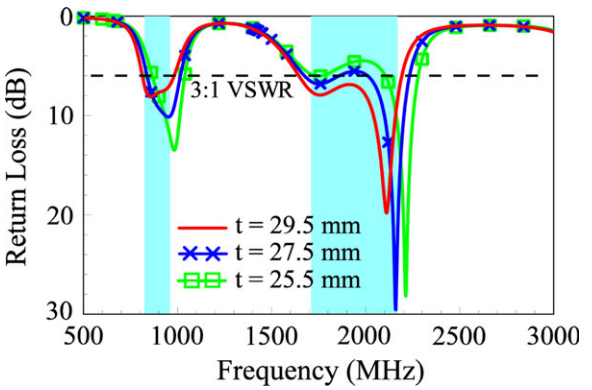

Figure 10 Simulated return loss as a function of the end-section length t of the monopole slot. [Color figure can be viewed in the online issue, which is available at wileyonlinelibrary.com]

Effects of tuning the end-section length t of the monopole slot on the performances of the proposed antenna are also analyzed. Figure 10 shows the simulated return loss as a function of the length t. It is seen that when the length t is varied, which causes the length variations of the monopole slot, the two excited slot modes (the first mode in the lower and upper bands) are affected. In addition, it is observed that the two resonant modes contributed by the PR slit (the second mode in the lower and upper bands) are also affected. This behavior is mainly because when the length t decreases, the shifting of the two excited slot modes to higher frequencies also causes shifting of the new resonances contributed by the PR slit to higher frequencies. Hence, the resonant modes contributed by the PR slit are also shifted to higher frequencies as shown in figure. The results indicate that proper selection of the dimensions of the monopole slot is also important in the proposed design.

4. CONCLUSION

Dual-band bandwidth enhancement using a PR slit for a simple folded monopole slot antenna has been shown. The proposed antenna has a planar structure occupying a small size of $10 \times 45 \times 0.8$ mm^3 and provides two wide operating bands to, respectively, cover the 824–960 and 1710–2170 MHz bands for the penta-band WWAN operation. The operating principle of the PR slit for dual-band bandwidth enhancement of the antenna's lower and upper bands has been discussed. Good radiation characteristics of the frequencies over the operating bands have also been observed. The proposed antenna is suitable to be applied in the tablet computer for the WWAN operation including the GSM850/900/1800/1900/UMTS bands.

REFERENCES

1. K.L. Wong, Y.W. Chang, and S.C. Chen, Bandwidth enhancement of small-size WWAN tablet computer antenna using a parallel-resonant spiral slit, IEEE Trans Antennas Propag 60 (2012), 1705–1711.
2. Y.W. Chi and K.L. Wong, Very-small-size folded loop antenna with a band-stop matching circuit for WWAN operation in the mobile phone, Microwave Opt Technol Lett 51 (2009), 808–814.
3. S.C. Chen and K.L. Wong, Low-profile, small-size WWAN handset antenna close integration with surrounding ground plane, Microwave Opt Technol Lett 54 (2012), 623–629.
4. F.H. Chu and K.L. Wong, Internal coupled-fed loop antenna integrated with notched ground plane for WWAN operation in the mobile handset, Microwave Opt Technol Lett 54 (2012), 599–605.
5. K.L. Wong and P.J. Ma, Small-size WWAN monopole slot antenna with dual-band band-stop matching circuit for tablet computer application, Microwave Opt Technol Lett 54 (2012), 875–879.
6. K.L. Wong and T.J. Wu, Small planar internal WWAN tablet computer antenna, Microwave Opt Technol Lett 54 (2012), 305–309.
7. K.L. Wong, Y.C. Liu, and L.C. Chou, Bandwidth enhancement of WWAN/LTE tablet computer antenna using embedded parallel resonant circuit, Microwave Opt Technol Lett 54 (2012), 426–431.
8. H. Wang, M. Zheng, and S.Q. Zhang, Monopole slot antenna, US Patent No. 6618020 B2, 2003.
9. P. Lindberg, E. Ojefors, and A. Rydberg, Wideband slot antenna for low-profile hand-held terminal applications, In: Proceedings of 36th European Microwave Conference (EuMC2006), Manchester, UK, 2006, pp. 1698–1701.
10. W.S. Chen and K.Y. Ku, Broadband design of a small non-symmetric ground λ/4 open slot antenna, Microwave J (2007), 110–120.
11. C. Hsieh, T. Chiu, and C. Lai, Compact dual-band slot antenna at the corner of the ground plane, IEEE Trans Antennas Propag 56 (2009), 3423–3426.
12. C.I. Lin and K.L. Wong, Printed monopole slot antenna for internal multiband mobile phone antenna, IEEE Trans Antennas Propag 55 (2007), 3690–3697.
13. C.H. Chang and K.L. Wong, Internal multiband surface-mount monopole slot chip antenna for mobile phone application, Microwave Opt Technol Lett 50 (2008), 1273–1279.
14. F.H. Chu and K.L. Wong, Simple folded monopole slot antenna for penta-band clamshell mobile phone application, IEEE Trans Antennas Propag 57 (2009), 3680–3684.
15. K.L. Wong and L.C. Lee, Multiband printed monopole slot antenna for WWAN operation in the laptop computer, IEEE Trans Antennas Propag 57 (2009), 324–330.
16. K.L. Wong and F.H. Chu, Internal planar WWAN laptop computer antenna using monopole slot elements, Microwave Opt Technol Lett 51 (2009), 1274–1279.
17. K.L. Wong, P.W. Lin, and C.H. Chang, Simple printed monopole slot antenna for penta-band WWAN operation in the mobile handset, Microwave Opt Technol Lett 53 (2011), 1399–1404.
18. K.L. Wong and P.W. Lin, Surface-mount WWAN monopole slot antenna for mobile handset, Microwave Opt Technol Lett 53 (2011), 1890–1896.
19. K.L. Wong, W.J. Chen, L.C. Chou, and M.R. Hsu, bandwidth enhancement of the small-size internal laptop computer antenna using a parasitic open slot for the penta-band WWAN operation, IEEE Trans. Antennas Propag 58 (2010), 3431–3435.
20. Available at: http://www.ansys.com/products/hf/hfss/, ANSYS HFSS, Ansoft, Pittsburgh, PA.
21. K.L. Wong and S.C. Chen, Printed single-strip monopole using a chip inductor for penta-band WWAN operation in the mobile phone, IEEE Trans Antennas Propag 58 (2010), 1011–1014.
22. C.L. Liu, Y.F. Lin, C.M. Liang, S.C. Pan, and H.M. Chen, Miniature internal penta-band monopole antenna for mobile phones, IEEE Trans Antennas Propag 58 (2010), 1008–1011.
23. C.T. Lee and K.L. Wong, Planar monopole with a coupling feed and an inductive shorting strip for LTE/GSM/UMTS operation in the mobile phone, IEEE Trans Antennas Propag 58 (2010), 2479–2483.
24. K.L. Wong, W.Y. Chen, and T.W. Kang, On-board printed coupled-fed loop antenna in close proximity to the surrounding ground plane for penta-band WWAN mobile phone, IEEE Trans Antennas Propag 59 (2011), 751–757.
25. F.H. Chu and K.L. Wong, Simple planar printed strip monopole with a closely-coupled parasitic shorted strip for eight-band LTE/GSM/UMTS mobile phone, IEEE Trans Antennas Propag 58 (2010), 3426–3431.
26. C.H. Chang and K.L. Wong, Printed λ/8-PIFA for penta-band WWAN operation in the mobile phone, IEEE Trans Antennas Propag 57 (2009), 1373–1381.
27. Y.W. Chi and K.L. Wong, Quarter-wavelength printed loop antenna with an internal printed matching circuit for GSM/DCS/

PCS/UMTS operation in the mobile phone, IEEE Trans Antennas Propag 57 (2009), 2541–2547.
28. A. Cabedo, J. Anguera, C. Picher, M. Ribo, and C. Puente, Multiband handset antenna combining a PIFA, slots, and ground plane modes, IEEE Trans Antennas Propag 57 (2009), 2526–2533.

STAR 16QAM/OOK BIDIRECTIONAL TRANSMISSION OVER A TDM-PON

Nikolaos Sotiropoulos, A. M. J. Koonen, and Huug de Waardt
COBRA Research Institute, Eindhoven University of Technology, P.O. Box 513, Eindhoven 5600 MB NL, The Netherlands; Corresponding author: n.sotiropoulos@tue.nl

Received 13 April 2012

ABSTRACT: *Transmission of Star 16QAM with differential detection has been demonstrated over a time division multiplexing (TDM)-PON. The multilevel downstream channel is operating at 10 Gb/s, while an OOK signal at 2.5 Gb/s is used for the upstream. Results show very good receiver sensitivity, indicating the modulation format's suitability for next-generation TDM-PONs.* © 2012 Wiley Periodicals, Inc.
Microwave Opt Technol Lett 55:45–47, 2013; View this article online at wileyonlinelibrary.com. DOI 10.1002/mop.27265

Key words: *direct detection; multilevel systems; optical fiber subscriber loops; optical modulation*

1. INTRODUCTION

The emergence of bandwidth-demanding applications like file sharing, High-definition television and social networking has fueled the deployment of fiber-based access networks across the world. The introduction of even more bandwidth-hungry services, such as 3D HDTV, telepresence, and cloud computing, means that the demand for higher bit rates will continue unabated [1].

To cope with the demand, the time division multiplexing (TDM)-PON community has developed a series of standards, with the most recent ones specifying 10 Gb/s operation [2]. Already, discussions are under way for next-generation PONs, with the key requirements being increased bit rate, increased splitting ratio, longer reach, and lower power consumption [3], while keeping the cost-effective advantage inherent in TDM-PONs.

The introduction of multilevel modulation formats, which can transmit multiple bits per symbol, can help future PONs to meet some of those requirements. With multilevel formats, optical and electrical components operating at a fraction of the bit rate can be used, leading to lower cost and power consumption. The reduced line rate will also remove the need for chromatic dispersion (CD) compensation, even for long-reach PONs. There is increased interest in the literature for coherent detection of optical multilevel signals in access networks, with focus on quadri-phase shift keying (QPSK) and QPSK-POLMUX [4, 5]. With this configuration, superior sensitivity can be achieved; however, coherent detection, especially with POLMUX, requires a large number of components, low-linewidth lasers, and extensive digital signal processing (DSP). In this article, four-bits-per-symbol downstream transmission is demonstrated with Star 16QAM and differential detection. Differential (incoherent) detection is advantageous in a PON, because it simplifies the receiver (no need for local oscillator) and greatly reduces the required DSP (no polarization demultiplexing or carrier and phase recovery). That way, cost-effective next generation TDM-PONs satisfying the network operators' requirements can be implemented. As a first proof of concept, the bit rate is set at 10 Gb/s. A simple directly modulated laser (DML) provides an upstream channel at 2.5 Gb/s.

2. STAR 16QAM

Differential phase-shift keying (DPSK) has been the most popular differential modulation format so far, encoding information on the phase difference between consecutive symbols. High-order DPSK formats, up to D8PSK, have been demonstrated [6]. If formats encoding four bits per symbol are desired, however, DPSK is unattractive, because its OSNR requirements increase rapidly with the constellation size [7]. To achieve higher spectral efficiency, an amplitude-shift keying (ASK) component must also be added. Several such formats have been proposed, with the most important being a combination of 2ASK-D8PSK (Star 16QAM) [7, 8], a combination of 4ASK-DQPSK [9], and phase-preintegrated 16QAM [10]. In this article, Star 16QAM has been selected, because it exhibits the best sensitivity out of the three [8].

The Star 16QAM constellation diagram consists of 16 points arranged in two rings of eight each. Information is encoded in the amplitude (one bit) and in the phase difference between consecutive symbols (the remaining three bits). The Star 16QAM systems that have been proposed in the literature [7, 8] create the multilevel optical signal using three or four modulators in series, each driven by binary electrical signals. The approach in this article is DSP-based, using multilevel electrical signals to drive a nested Mach–Zehnder modulator pair. As silicon DSP chips, digital-to-analog and analog-to-digital converters become available at high speeds [11], they can be utilized to reduce complexity in the optical domain and provide additional functionalities (signal predistortion, electronic CD compensation). The differential encoding of the data is also performed in the DSP.

A receiver that is capable of detecting the Star 16QAM signal consists of a pair of asymmetric Mach–Zehnder delay interferometers, followed by balanced photodetectors, and a photodiode. Phase demodulation takes place in the interferometers, where the differential encoding is canceled out by the beating of every symbol, s_n, with its delayed (by one period) version, resulting after balanced detection to the metrics $\mathrm{Re}\{s_n \cdot \overline{s_{n-1}}\}, \mathrm{Im}\{s_n \cdot \overline{s_{n-1}}\}$. That way, the phase difference between consecutive symbols is recovered, which corresponds to the original phase information of the symbol. The single photodiode is used to detect the amplitude of the multilevel signal, which is then combined with the phase information to reconstruct the original symbol.

3. EXPERIMENTAL SET-UP AND RESULTS

To evaluate of the scheme described in the previous section, an experimental set-up has been developed and is shown in Figure 1. The differential encoding of the downstream data (100k symbols long), as well as the predistortion to compensate for the modulators' nonlinear transfer function, is being done offline in Matlab, and the resulting waveforms are loaded to an arbitrary waveform generator (AWG). The AWG creates the analog waveforms at 5 Gsam/s, which are then amplified and drive an IQ modulator. The IQ modulator consists of a nested pair of Mach–Zehnder modulators, with a phase shift of 90° in one arm to create the quadrature component. A continuous wave light at 1550 nm is provided by an external cavity laser with a linewidth of 100 kHz. The created Star 16QAM signal is then launched